Colloid Polym Sci 279:872–878 (2001)

ORIGINAL CONTRIBUTION

J.-H. Mu
G.-Z. Li

Rheology of viscoelastic anionic micellar solutions in the presence of a multivalent counterions

Received: 23 November 2000
Accepted: 31 January 2001

J.-H. Mu (✉) · G.-Z. Li
Key Laboratory for Colloid and Interface Chemistry of State Education Ministry
Shandong University, Jinan 250100
China
e-mail: mujianhai@263.net
Tel.: +86-531-8564750

Abstract The growth and structure of anionic micelles sodium dodecyl trioxyethylene sulfate (SDES) in the presence of a multivalent counterion, Al^{3+}, were investigated by means of rheological methods and the technique of freeze-fracture transmission electron microscopy. It was found that wormlike micelles and network structures could be formed in SDES/$AlCl_3$ aqueous micellar solutions, according to the measurements of the zero-shear viscosity, the complex viscosity and the dynamic moduli (storage modulus and loss modulus), and the application of the Cox–Merz rule and a Cole–Cole plot. The cyclic shear test, the plateau modulus and the relaxation time were also studied to express the rheological properties of the wormlike micellar solutions. The structure was of a character of a nonlinear viscoelastic fluid and departed from the simple Maxwell model.

Key words Rheology · Viscoelasticity · Wormlike micelles · Sodium dodecyl trioxyethylene sulfate

Introduction

The study of rheology is vital in many industrial applications, including food emulsions, cosmetics, paints, agrochemicals, pharmaceuticals, bitumen emulsions, inks and paper coatings, adhesives and many household products. The rheological properties are a function of both the structural arrangement of particles and various interaction forces which operate in the system. It is now well known that the addition of salt to aqueous cationic surfactant weakens electrostatic interactions and enhances micellar growth, in which the spherical surfactant micelles undergo a transition to larger rodlike aggregations with a molar weight of about 10^6, named wormlike micelles [1–9]. They have high surface activity, high viscosity and the property of shear thinning, which make them have such wide uses in many fields that people pay more and more attention to them. However, for anionic micelles, there are fewer reports.

Recently, we have been interested in the micellar growth induced by an increase in the amount of anionic surfactant, sodium dodecyl trioxyethylene sulfate (SDES), and salts, $AlCl_3$, $CaCl_2$, KBr, NaCl, etc., in systems where wormlike micelles or network structures are formed. In this work, rheological methods and freeze-fracture transmission electron microscopy (FF-TEM) were applied to investigate the formation and viscoelasticity of wormlike micelles and network structures in anionic surfactant SDES aqueous solutions in the presence of the multivalent counterion electrolyte $AlCl_3$. Some interesting and notable conclusions will enrich the theory and application of wormlike micelles.

Materials and methods

Materials

The solutions studied in this work were made of the anionic surfactant SDES, with the formula $CH_3(CH_2)_{11}(OCH_2CH_2)_3$-$OSO_3Na$, and the electrolyte $AlCl_3$, which were both analytical reagent grade. All the micellar solutions were prepared by using deionized water and were left to stand for 2 days to reach equilibrium, and there were no air bubbles in the solutions.

Rheological measurements

Rheological measurements were made with a Haake RS 150 rheometer at a constant temperature of 30 ± 0.2 °C. A cone–plate sensor was used, with a diameter of 20 mm and a cone angle of 0.5°. The sample thickness in the middle of the sensor was 0.03 mm. The viscosity, η, and stress, σ, of the samples were obtained with steady-shear measurements. Frequency-sweep measurements were performed at a given stress, σ_0, (chosen in the linear domain where the amplitude of the deformations is very low) in the frequency (ω) region varying from 0.06 to 100 rads^{-1}.

In the case of a Maxwell fluid, the storage modulus, G', the loss modulus, G'', and the complex viscosity, $|\eta^*|$, are given by the following equations [10]:

$$G'(\omega) = G_0 \frac{\omega^2\tau^2}{1+\omega^2\tau^2} \quad , \tag{1}$$

$$G''(\omega) = G_0 \frac{\omega\tau}{1+\omega^2\tau^2} \quad , \tag{2}$$

$$|\eta^*(\omega)| = \frac{(G'^2 + G''^2)^{\frac{1}{2}}}{\omega} \quad , \tag{3}$$

with the relaxation time

$$\tau = \frac{\eta_0}{G_0} \quad . \tag{4}$$

Here η_0 is the zero-shear-rate viscosity and the elastic modulus, G_0, is measured at high frequency where G' reaches a plateau. Also of interest is a linear plot of G'' versus G' which reveals the semicircle (Cole–Cole) characteristic of a Maxwell fluid, which is expressed as Eqs. (5) and (6).

$$\frac{G'}{G''} = \omega\tau \quad , \tag{5}$$

$$G''^2 + \left(G' - \frac{G_0}{2}\right)^2 = \left(\frac{G_0}{2}\right)^2 \quad . \tag{6}$$

Freeze-fracture transmission electron microscopy

The FF-TEM investigation [8, 9, 11] was carried out using a FF apparatus (Eiko Model FD-2A) on a nitrogen-cooled support and a TEM (Jeol model JEM-1200EX). The procedure comprises the following main steps: sample preparation, freezing of the specimen, fracturing about 30 min at a high vacuum of 10^{-5} Pa from −140 to −95 °C, replication of the fracture face with Pt–C vapor, and finally transmission electron microscopic investigation of the replicas.

Results and discussions

The formation of wormlike micelles

The zero-shear viscosity, η_0, of SDES/$AlCl_3$ solutions was measured as a function of the surfactant and salt concentrations, respectively, as shown in Fig. 1. In Fig. 1a, on increasing the $AlCl_3$ concentration with a fixed SDES concentration of 0.08 M, the viscosity shows first a slow increase and then a sharp increase at 0.40–0.50 M $AlCl_3$ until a maximum of 1.9 Pas at a salt concentration of 0.80–0.90 M, and finally decreases dramatically: This behavior is expected. It is similar to

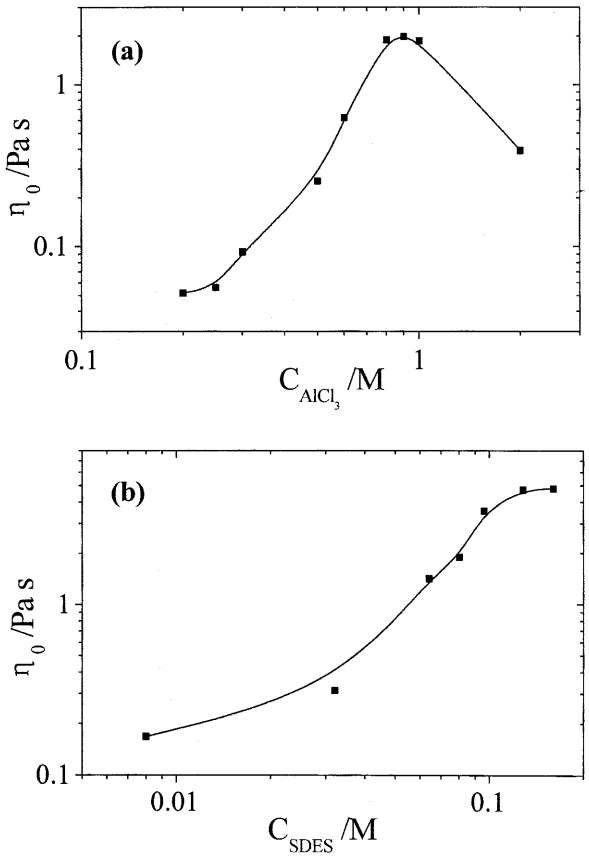

Fig. 1a, b Zero-shear viscosity, η_0, as a function of $AlCl_3$/dodecyl trioxyethylene sulfate (*SDES*) concentrations. **a** [SDES] = 0.08 M; **b** [$AlCl_3$] = 0.80 M

the behavior obtained in several aqueous surfactant/salt systems [4] and is explained by connections which result from the formation and breaking of wormlike micelles. It is generally admitted that at fixed surfactant concentration, an increase in the salt content leads to a micellar growth, because of the enhanced screening of the interactions. With a low salt content, rodlike micelles may be formed and grow, which cannot show an evident increase in the viscosity of solutions. When the length of the rodlike micelles has increased further so that they are flexible and can curve freely, the micelles become wormlike, which can result in a rapid increase in viscosity; however, if the salt concentration is very high, the wormlike micelles may break into several pieces [4], and at the same time, the effect of salting-out becomes so obvious that the content of surfactant in the bulk solution decreases, and so the viscosities of the samples become lower.

The effect of the surfactant concentration on the zero-shear viscosity of 0.80 M $AlCl_3$ solutions is illustrated in Fig. 1b. The curves can be divided into three domains: at lower SDES concentration (below 0.04 M), η_0 shows little change and then increases until a maximum of

4.8 Pas at an SDES content of 0.12 M; it remains constant after that point. This can also be explained from the viewpoint of micellar growth. A lower SDES content only leads to an increase in the size and number of rodlike micelles, and the increase in the length of the micelles and the formation of wormlike micelles and entangled network structures occurs at a certain surfactant concentration.

According to the results of Fig. 1, the sample 0.08 M SDES/0.80 M $AlCl_3$ can be investigated further to ensure the formation of wormlike micelles and network structures. FF–TEM was applied to make sure that such structures were formed in the sample. The application of FF-TEM to the microstructure of complex fluids directly, like microemulsions, wormlike micelles, vesicles and dilute lamellar systems, has been demonstrated recently [8, 9, 11]. The electron micrographs of the vitrified sample are shown in Fig. 2. Figure 3a is an image of the sample with a magnification 2×10^4 showing lots of flexible wormlike structures, which are wormlike micelles. Some micelles entangle with each other and form weak network structures. It also can be observed that many "micelle faces" appear owing to the different arrangement of wormlike micelles, with the same direction in a "micelle face". The well-arranged structure of wormlike micelles would be destroyed to a mixed and disorderly orientation by shearing, so more and more micelles can entangle further and the relatively obvious network structure will be formed.

Figure 2b is an image with a magnification 4×10^4, in which the flexible wormlike micelles and local network structures can be observed distinctly. The micelles are approximately 10 nm in diameter and 100–200 nm in length in general, and the longest "worm" is about 400 nm. The ratio of the length and the diameter is at least larger than 10. In addition, the existence of some spherical and rodlike particles in the image shows that the wormlike micelles have not been formed completely in the sample, resulting in the lower zero-shear viscosity

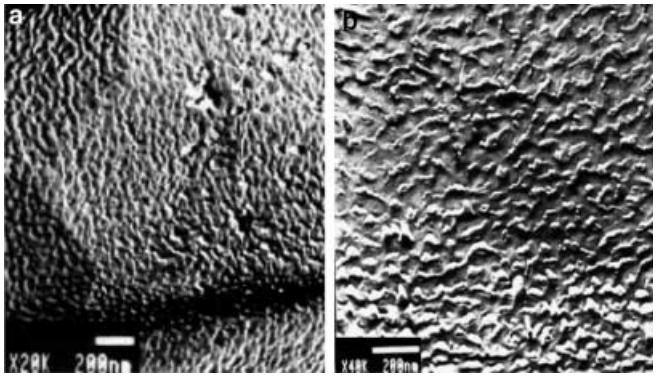

Fig. 2a, b Freeze-fracture transmission electron microscopy micrographs of 0.08 M SDES/0.80 M $AlCl_3$ solution (*bars* = 200 nm)

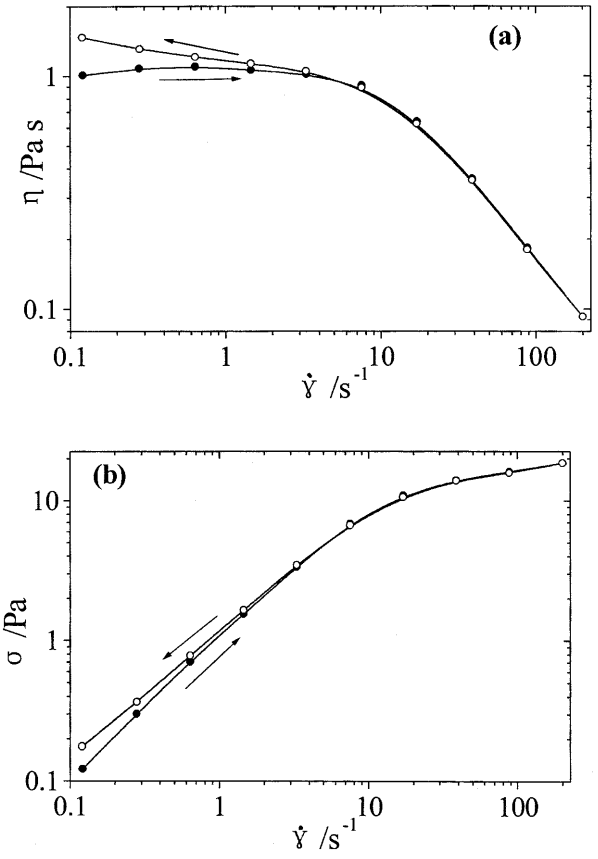

Fig. 3a, b Cyclic-shear test for 0.08 M SDES/0.80 M $AlCl_3$ solution. **a** Flow curve for viscosity versus shear rate; **b** flow curve for stress versus shear rate

(about 2.0 Pas) of the solution. A reasonable reason is that the concentration of surfactant in the sample is so low that the interesting structure cannot be formed perfectly.

Flow curves of the sample

Typical flow curves of the sample 0.08 M SDES/0.80 M $AlCl_3$, obtained from the cyclic shearing test with a range of shear rates from 0.1 to 200 s^{-1} are shown in Fig. 3. The relationship between η and $\dot{\gamma}$ is shown in Fig. 3a, and that between σ and $\dot{\gamma}$ in Fig. 3b. The down curve does not overlap with the up one completely, indicating the partial irreversible destruction of the internal structure. The up curve indicates viscosity or stress values lower than those corresponding to the down curve at low shear rates, a typical rheopectic characteristic [12]. With the increase in shear rates, the solution first shear flows nearly as a Newtonian fluid, and the slope of the double logarithmic plot of stress against shear rate is approximately 1, which is consistent

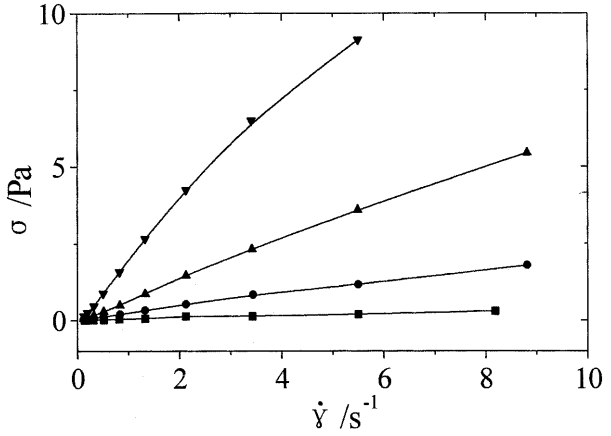

Fig. 4 Shear stress at low shear rate for solutions with $AlCl_3$ 0.80 M and SDES (■) 0.064M, (●) 0.080M, (▲) 0.096M, (▼) 0.128M

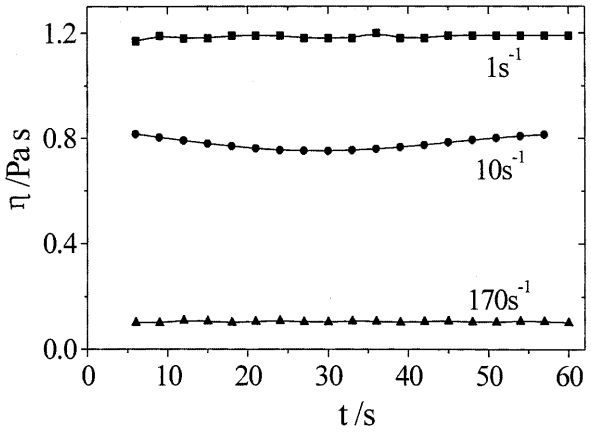

Fig. 5 Viscosity–time curves of 0.08 M SDES/0.80 M $AlCl_3$ solution at different shear rates

with the viscosity of about 1.0 Pas. However, at a characteristic rate, the shear stress reaches a maximum value and becomes much less dependent on the shear rate, and so the phenomenon of shear thinning occurs. According to the conclusions of FF-TEM in Fig. 2, the wormlike micelles can entangle further and form the local network structures in the case of the lower shear rate in the up curve, but the shear-induced structures may not be restored to their original configuration in the cyclic shear test, which results in the higher values of viscosity and stress in the down curve.

In order to investigate the type of the wormlike micellar solutions studied, the stress at low shear rates (0–8 s^{-1}) is shown in Fig. 4. The curves indicate that the relationship between stress and shear rate is linear and that the slope gradually becomes greater as the surfactant concentration increases. There is almost no stress yield value for all the samples, which shows that the wormlike micellar solutions behave as a pseudoplastic fluid [10]. The viscosity of the sample as a function of time is shown in Fig. 5 at three different shear rates: 1, 10 and 170 s^{-1}. The higher the shear rate, the lower the viscosity, which has already been discussed for Fig. 3. It can also be seen that the viscosity is a constant and is less dependent on time if the shear rate is fixed. There is not the phenomenon of the shear-induced structure transition for this condition.

The viscoelasticity of wormlike micelles

Before carrying out any oscillatory measurements each sample should be checked to ensure it is within the linear viscoelastic region where the complex modulus (G^*) or the damping factor ($\tan\delta = G''/G'$) is independent of the applied stress [13, 14]. Typical results of G^* and $\tan\delta$ of the sample 0.08 M SDES/0.80 M $AlCl_3$ solution as a function of the stress at a constant frequency (1.0 Hz) can be seen in Fig. 6. It can be stated that most of the samples have linear viscoelasticity up to about 10 Pa. For subsequent dynamic experiments we chose a stress value of 1.0 Pa.

It has been suggested that for solutions with wormlike micelles and network structures, the steady-shear viscosity (η) and the magnitude of the complex viscosity ($|\eta^*|$) superimpose closely at equivalent values of the shear rate ($\dot{\gamma}/s^{-1}$) and angular frequency (ω/rads^{-1}), i.e. these solutions obey the Cox–Merz rule [15]. If the structure can survive small oscillatory deformation but may be ruptured by large deformation, $|\eta^*|$ is significantly larger than η and so these solutions tend to depart from the Cox–Merz superposition. The shear-rate dependence of the η and the frequency dependence of $|\eta^*|$ are shown in Fig. 7 for the sample studied. It is shown that η and $|\eta^*|$ are in some agreement with each

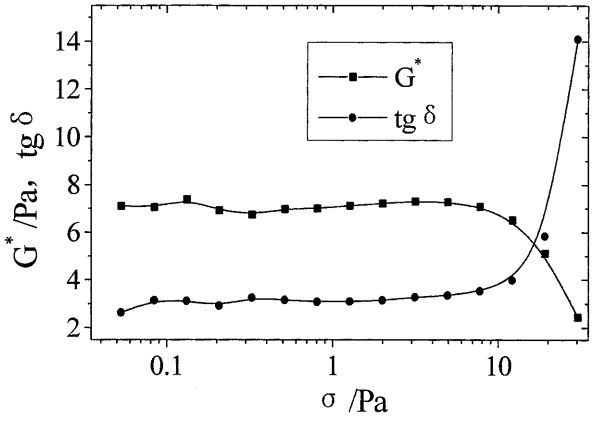

Fig. 6 The complex modulus (G^*) and the damping factor ($\tan\delta = G''/G'$) of 0.08 M SDES/0.80 M $AlCl_3$ solution as a function of the applied stress (σ) at a constant frequency (1.0 Hz)

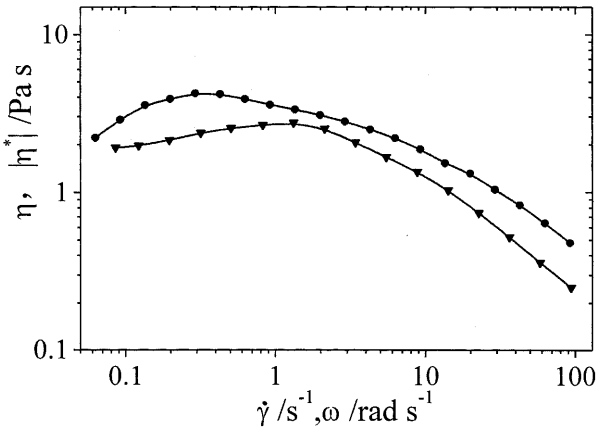

Fig. 7 Shear-rate dependence of the steady-shear viscosity (▼) and the frequency dependence of the absolute value of the complex viscosity (●) for 0.08 M SDES/0.80 M $AlCl_3$ solution

other, and $|\eta^*|$ is slightly larger than η at all shear rates (frequencies). It can be concluded that the wormlike micelles and network structures have already been formed in the system, but the structures are not evident or steady, and there are probably some small wormlike micelles and local entanglements.

It is also shown in Fig. 7 that the shear viscosity increases slightly at first (shear thickening) and decreases dramatically after reaching the maximum value as the shear rate is further increased (shear thinning), which indicates an evident departure from the simple Maxwell model and shows a nonlinear viscoelasticity or a non-Newtonian flow behavior [16]. It can be explained as follows. In a lower shear rate range, some micelles and surfactant molecules can aggregate and entangle further and the viscosity of sample will increase; on the other hand, the micelles can be stretched in the flow profile if the shear rate is high, which results in a decrease in viscosity [13]. The results obtained from the FF-TEM micrographs can also lead to this conclusion.

G' and G'' can describe the viscoelasticity of the solutions [16, 17]. They are plotted against the angular frequency for the 0.08 M SDES/0.80 M $AlCl_3$ system in Fig. 8a. The curve describing G' and G'' crosses at about $\omega = 20.0$ rads^{-1} as the rate increases, indicating that the material is more elastic than viscous at high frequencies, and G' and G'' above the intersection tend to level off and approach plateau values.

It is sometimes difficult to determine how "good" a Maxwell model fits the data from plots of G' and G'' versus ω. A Cole–Cole plot (plot of G'' as a function of G') provides a better picture of how well the data correspond to a single relaxation time Maxwell model, which reveals the semicircle characteristic of a Maxwell fluid [16]. Figure 8b shows a Cole–Cole plot from the data presented in Fig. 8a. The data points do not fit on a

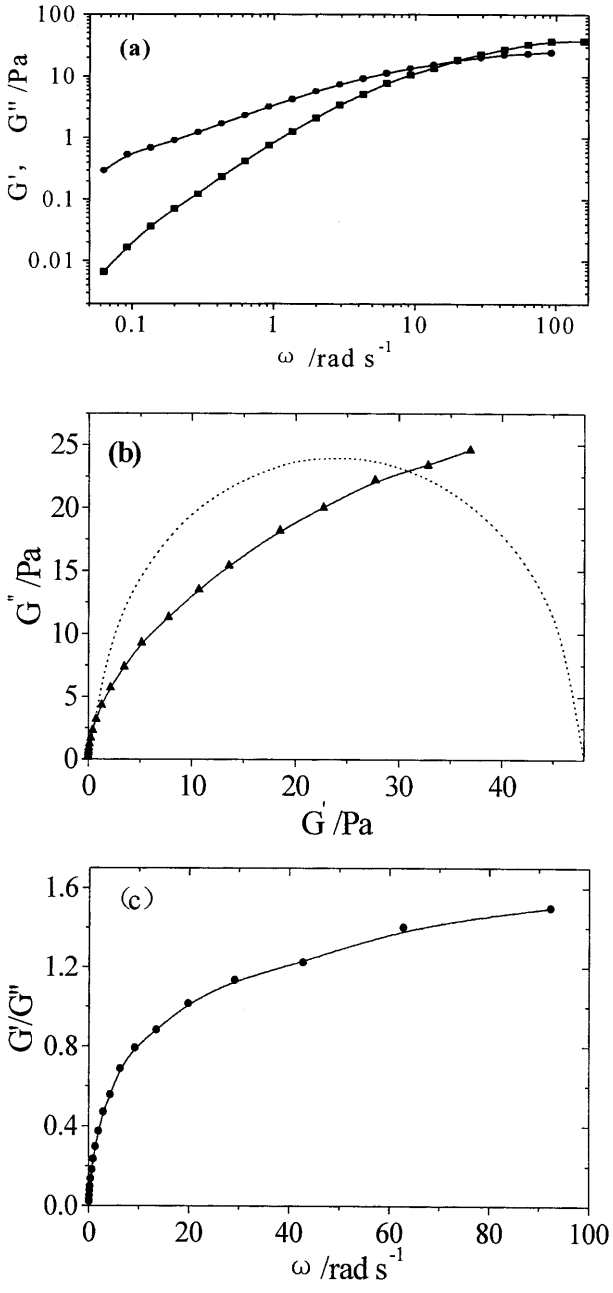

Fig. 8 The storage modulus (■) and the loss modulus (●) **a** as a function of the angular frequency, **b** Cole–Cole plot and c G'/G''–ω curve for 0.08 M SDES/0.80 M $AlCl_3$ solution

semicircular curve (dotted line) from Eq. (6), in agreement with the aforementioned conclusion that these data are not well fit by a simple Maxwell model.

Figure 8c shows the ratio of G' and G'' as a function of the angular frequency, in order to make a further determination of how "good" the Maxwell model and the linear viscoelasticity fit the wormlike micellar solution as well as the Cole–Cole plot. According to Eq. (5),

for a linear viscoelastic fluid the ratio has a linear relationship with frequency. Figure 8c indicates that the curve is almost linear except at an intermediate angular frequency, notwithstanding the slope at low frequency, which is much larger than that at high frequency, which shows that the relaxation time of the sample is not simple and that the process of relaxation is much slower at low frequency than that at high frequency.

Although the wormlike micellar solution is not a Maxwell fluid with a simple relaxation time, the relaxation can be expressed by the so-called apparent relaxation time, τ_a, obtained from Eq. (4) for a nonlinear viscoelastic fluid. Double logarithmic dependences of the shear modulus (G_0, plateau modulus) and τ_a on the surfactant molar concentration in the solutions with 0.80 M $AlCl_3$ are shown in Figs. 9 and 10. In the range of SDES concentrations from about 0.04 M, where the wormlike micelles begin forming, to about 0.12 M, where the wormlike micelles form completely according to the results obtained from Fig. 1b, the slopes of the best linear fits to the data are 1.0 for G_0 and 1.2 for τ_a. There are also theoretical predictions. The closest agreement is observed with the exponent value for G_0 and τ_a in a model developed by Cates [18]. In this model, the wormlike micelles are taken as linear and flexible. The structural relaxation is determined not only by the diffusion, but also by the dissociation/recombination of aggregates. The power law for the plateau modulus and the relaxation time is in the form of

$$G \sim c^{9/4} \quad , \tag{7}$$

$$\tau_a \sim c^{5/4} \quad , \tag{8}$$

where c is the surfactant concentration. It is obvious that the increasing exponent of G_0 departs from the theoretical value, 2.25, indicating the lower elastic property of the sample studied compared with the ideal structures and some cationic and nonionic wormlike micelles [4, 19]. The evolution of the relaxation time shows two breaks in the slope in Fig. 10, which corresponds to the concentrations at the beginning and the end of the formation of the wormlike micelles in the sample, respectively, consistent with the results in Fig. 1b. The relaxation time increases slowly in domain 1 with an exponent of 0.16, because there is no obvious change in η_0 and G_0 at such a low concentration of SDES. At the moment of the formation of the wormlike micelles, the η_0 increases faster compared with the G_0, resulting in a sudden increase in the relaxation time with an exponent of 1.2 in domain 2, being in good agreement with the theoretical prediction, 1.25. After the wormlike micelles form completely, an increase in the surfactant concentration will only result in an increase in the elastic property, i.e. the G_0, and the viscosity of the solution changes little (Fig. 1b), which leads to a decrease in the relaxation time with an exponent of −0.50 at high concentrations in domain 3.

According to the results obtained from Fig. 3b, there is a stress plateau (σ_∞) for the wormlike micellar solutions at high shear rates. Hoffmann et al. [2] provided a theoretical description from fitting procedures for this condition:

$$\sigma(\dot{\gamma}) = \frac{\eta_0 \dot{\gamma}}{(1 + 2\dot{\gamma}^2\tau^2)^{0.5}} \quad . \tag{9}$$

For $\dot{\gamma}\tau \gg 1$, the maximum of the stress

$$\sigma_\infty = \frac{\eta_0}{2^{0.5}\tau} = \frac{G_0}{2^{0.5}} \quad . \tag{10}$$

This is an interesting result because it offers the opportunity to measure the equilibrium shear modulus from steady-shear shear stresses. Figure 11 shows the approximately linear relationship between G_0 and σ_∞ for the

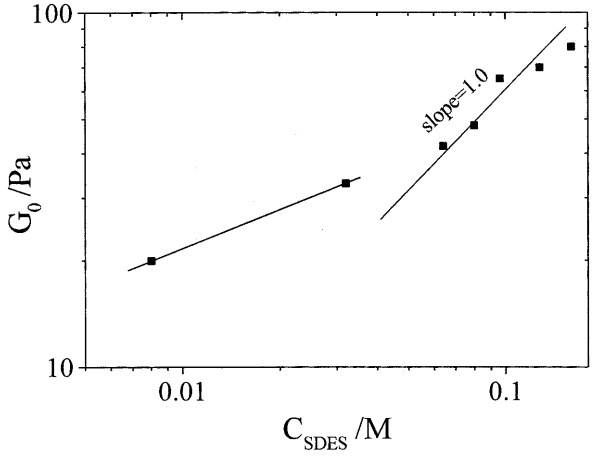

Fig. 9 The shear modulus (G_0) as a function of the surfactant concentration for solutions with 0.80 M $AlCl_3$

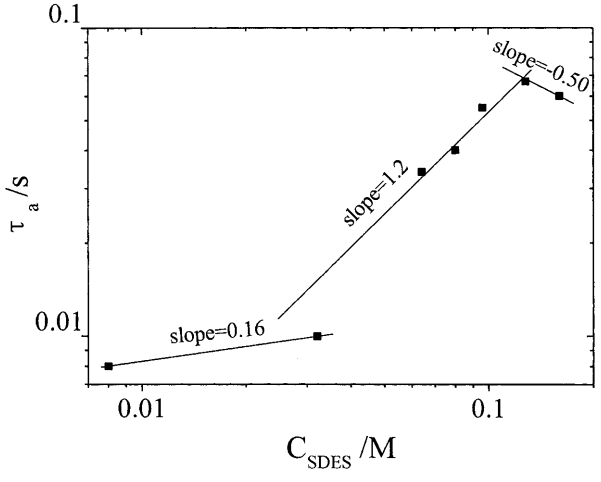

Fig. 10 The apparent relaxation time, τ_a, as a function of SDES concentration for solutions with 0.80 M $AlCl_3$

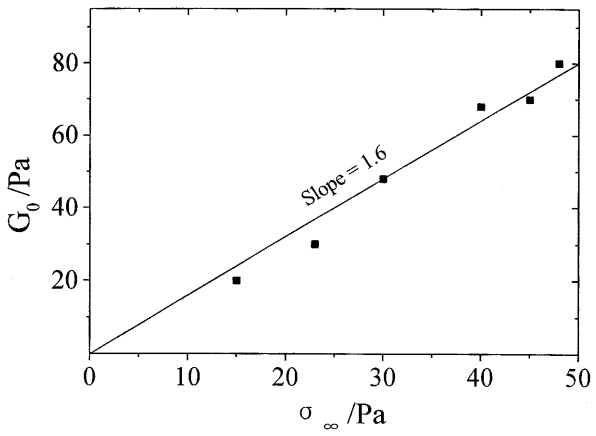

Fig. 11 G_0 as a function of the maximum shear stress for solutions with different SDES concentrations and 0.80 M $AlCl_3$

wormlike micellar solutions, though the slope is about 1.6 not $2^{0.5}$ (1.4), which indicates the G_0 can be obtained from the plateau value of the stress at high shear rates according to an appropriate theoretical description.

Conclusion

Wormlike micelles and local network structures were obtained for samples with the anionic surfactant SDES and multivalent counterion electrolyte $AlCl_3$ fixed in a proper concentration according to rheological measurements and FF-TEM micrographs. The characteristics of a pseudoplastic fluid and the shear-induced structures not restoring to their original configuration were acquired from the steady-shear experiments, i.e. cyclic-shear test, shear-stress measurements and viscosity–time curves. The Cox–Merz rule and a Cole–Cole plot show the rheological behavior of the nonlinear viscoelasticity, the departure from the Maxwell model and a relaxation time which is not simple. The G_0 and τ were also investigated to express the rheological properties of the wormlike micellar solutions.

Acknowledgements Financial support of this work by the National Natural Science Foundation of China (grant no. 29973023) and further support by the Research Institute of Exploration & Development, Daqing Petroleum Administrative Bureau of China are gratefully acknowledged.

References

1. Rehage H, Hoffmann H (1988) J Phys Chem 92:4712–4719
2. Hoffmann H, Rehage H, Rauscher A (1992) In: Chen H et al (eds) Statics and dynamics of strongly interacting colloids and supramolecular aggregates in solution. Fliver, Netherlands, pp 493–510
3. Berret JF (1997) Langmuir 13:2227–2234
4. Aït Ali A, Makhloufi R (1999) Colloid Polym Sci 277:270–275
5. Haas S, Hoffmann H, Thunig C, Hoinkis E (1999) Colloid Polym Sci 277:856–867
6. Kim WJ, Yang SM (2000) Langmuir 16:6084–6093
7. Zhang WC, Li GZ, Shen Q, Mu JH (2000) Colloids Surf A 170:59–64
8. Clausen TM, et al (1992) J Phys Chem 96:474–484
9. Hoffmann H, Thunig C, Schmiedel P (1994) Tenside Surfactants Deterg 31:389–400
10. Zana R (1987) In: Zana R (ed) Surfactants solutions: new methods of investigation. Dekker, New York, pp 209–240
11. Bolzinger-Thevenin MA, Grossiord JL, Poelman MC (1999) Langmuir 15:2307–2315
12. Alcantara MR, Vanin JA (1995) Colloids Surf A 97:151–156
13. Karlson L, Nilsson S, Thuresson K (1999) Colloid Polym Sci 277:798–804
14. Németh Z, et al (1998) Colloids Surf A 45:107–119
15. Miyoshi E, Nishinari K (1999) Colloid Polym Sci 277:727–734
16. Khatory A, et al (1993) Langmuir 9:1456–1464
17. Schulte J, Enders S, Quitzsch K (1999) Colloid Polym Sci 277:827–836
18. Cates ME (1990) J Phys Chem 94:371–375
19. Shchipunov YA, et al (1999) J Colloid Interface Sci 211:81–88